Breakdown of intermediate-range order in liquid $GeSe_2$ at high temperatures

2000 J. Phys.: Condens. Matter 12 L697

(http://iopscience.iop.org/0953-8984/12/46/102)

J. Phys.: Condens. Matter **12** (2000) L697–L704. Printed in the UK PII: S0953-8984(00)17134-6

LETTER TO THE EDITOR

Breakdown of intermediate-range order in liquid $GeSe_2$ at high temperatures

C Massobrio†, F H M van Roon‡, Alfredo Pasquarello§ and S W De Leeuw‡

† Institut de Physique et de Chimie des Matériaux de Strasbourg, 23 rue du Loess, F-67037 Strasbourg, France

‡ Department of Applied Physics, Lorentzweg 1, 2628 CJ Delft, The Netherlands

§ Institut Romand de Recherche Numérique en Physique des Matériaux (IRRMA), Ecole Polytechnique Fédérale de Lausanne (EPFL), PPH-Ecublens, CH-1015 Lausanne, Switzerland

Received 15 September 2000, in final form 25 October 2000

Abstract. The structure of liquid $GeSe_2$ at $T = 1373$ K has been investigated by first-principles molecular dynamics. The calculated total neutron structure factor is in good agreement with recent experimental data. We found that the disappearance with increasing temperature of the first sharp diffraction peak (FSDP) in the total neutron structure factor is due to an increase of short-range chemical disorder. At $T = 1373$ K various bonding configurations coexist in close amounts, such as the Ge–$GeSe_3$, Ge–$GeSe_2$ and Se–$SeGe_2$ motifs. This contrasts with the behaviour of liquid $GeSe_2$ at $T = 1050$ K, for which more than half of the Ge atoms are four-fold coordinated to Se atoms in regular $GeSe_4$ tetrahedra. Our result correlates the appearance of the FSPD in disordered AX_2 network-forming materials to the *predominant* presence of AX_4 subunits.

Liquid and glassy $GeSe_2$ are characterized by the occurrence of intermediate-range order (IRO) on length scales larger (5–12 Å) than those typical of nearest neighbour distances [1]. A typical manifestation of IRO is the first sharp diffraction peak (FSDP) appearing in the total neutron structure factor at short wavevectors (~ 1 Å^{-1}) [2–6]. This peak, found in the amorphous phase of $GeSe_2$, survives on melting with little modification of its intensity and position [1]. The atomic structure of molten [7] and glassy [8] $GeSe_2$ has been investigated by Salmon and coworkers via a partial-structure-factor analysis carried out using the method of isotopic substitution in neutron diffraction. The building blocks of these networks are the $GeSe_4$ tetrahedra, which are connected via corner- and edge-sharing configurations, the chemical order being broken by the existence of homopolar Ge–Ge and Se–Se bonds.

It is of interest to establish whether clues about the microscopic origin of the FSDP and the concomitant IRO in liquid $GeSe_2$ can be gained by following the evolution of the neutron structure factors when the temperature is raised well above the melting point, $T_m = 1015$ K. Towards this goal, a set of measurements of the total structure factors of liquid $GeSe_2$ has very recently been performed [9] at three temperatures, $T = 1073$ K, $T = 1273$ K, $T = 1373$ K. The results show that the FSDP, present at $T = 1073$ K, is very much reduced at the highest temperature. Despite this drastic change, the behaviour of the total pair distribution function $G_T(r)$ may suggest that the short-range order does not vary significantly upon increasing the temperature [9]. By assuming that the first peak of $G_T(r)$ accounts for Ge–Se correlations alone, a mean coordination number close to four was obtained in [9]. Although this number indicates that the $GeSe_4$ tetrahedron remains the dominant structural motif up to $T = 1373$ K, the lack of a full partial structure factor analysis prevents an unambiguous picture of the atomic structure from being achieved.

0953-8984/00/460697+08$30.00

Changes occuring in the structure of the liquid chalcogen mixture As_2Se_3 for increasing temperature have recently been investigated via first-principles molecular dynamics simulations [10, 11]. These studies have provided convincing evidence of the existence of a transition from a network to a two-fold chain-like arrangement. This approach appears ideally suited to complement the experimental results on high-temperature liquid $GeSe_2$ presented in [9] and achieve a better description of its structure. In this context, we recall that atomistic simulations have been performed on liquid $GeSe_2$ at temperatures close to the melting point, within different theoretical schemes [12–15]. In particular, the total neutron structure factor of liquid $GeSe_2$ obtained via first-principles molecular dynamics [14] was found to be in excellent agreeement with the experiments and the FSDP accurately reproduced.

In this work we investigate the short and intermediate-range order of liquid $GeSe_2$ at high temperatures via first-principles molecular dynamics. Our results for the total structure factor are in good agreement with the data of [9] and, in particular, they are consistent with the observed breakdown of intermediate-range order. Calculation of the average coordination numbers shows that the disappearance of the FSDP is related to a marked decrease in the number of $GeSe_4$ tetrahedra in the network. These changes are accompanied by an enhancement of three-fold bonding configurations and homopolar contacts. A comparative analysis with the results obtained for liquid $GeSe_2$ at $T = 1050$ K [14] highlights the relationship between the appearance of the FSDP in the total structure factor and the existence of a predominant structural motif, the AX_4 tetrahedron.

Our simulations are performed at constant volume, with the electronic structure described within density functional theory and evolving self-consistently during the motion [16]. As in previous work on liquid $GeSe_2$ at $T = 1050$ K [14] a generalized gradient approximation (GGA) for the exchange and correlation energy was adopted [17]. Details on the method of calculation have been given in recent publications on liquid $GeSe_2$ [14] and $GeSe_4$ [18]. In particular, the parameters relating to the integration of the equations of motion are the same as those of [14]. Our system consists of a stoichiometric composition of 120 atoms in a periodically repeated cubic cell of side 15.504 Å, corresponding to the experimental density [19] of the liquid at $T = 1373$ K. This means that, from the point of view of the implementation, the present simulations differ from those presented in [14] only by a different density (i.e. volume of the simulation cell) and a corresponding different temperature. The wave functions are expanded at the Γ point of the supercell on a plane wave basis set defined by an energy cutoff of 20 Ry. As an initial configuration we selected one previously obtained for the liquid at $T = 1050$ K by rescaling the coordinates to the desired density. After an initial trajectory lasting 10 ps at $T = 1050$ K, the temperature was raised to $T = 1373$ K and the system left to evolve for 1.5 ps. During the first part the atoms moved a distance close to 6 Å, thereby ensuring that the finally attained configuration keeps no memory of the initial condition. After the equilibration period, the actual data collection was taken over a period of 8 ps.

In figure 1 we display the measured and calculated total neutron structure factor $S_T(k)$ at $T = 1050$ K and $T = 1373$ K. In terms of the Faber–Ziman [20] partial structure factors this quantity reads

$$S_T(k) = \langle b\rangle^{-2}\{c_{Ge}^2 b_{Ge}^2[S_{GeGe}(k)-1]+2c_{Ge}b_{Ge}c_{Se}b_{Se}[S_{GeSe}(k)-1]+c_{Se}^2 b_{Se}^2[S_{SeSe}(k)-1]\}+1 \quad (1)$$

where $\langle b\rangle = (c_{Ge}b_{Ge} + c_{Se}b_{Se})$. In equation 1 c_α, and b_α denote the atomic fraction and the coherent scattering length of chemical species α, which are $b_{Ge} = 8.185$ fm and $b_{Se} = 7.97$ fm. The results obtained at $T = 1050$ K demonstrated that our model reproduces accurately at that temperature both the short- and intermediate-range distances [14]. The level of agreement between theory and experiment is less satisfactory at $T = 1373$ K, in particular in between

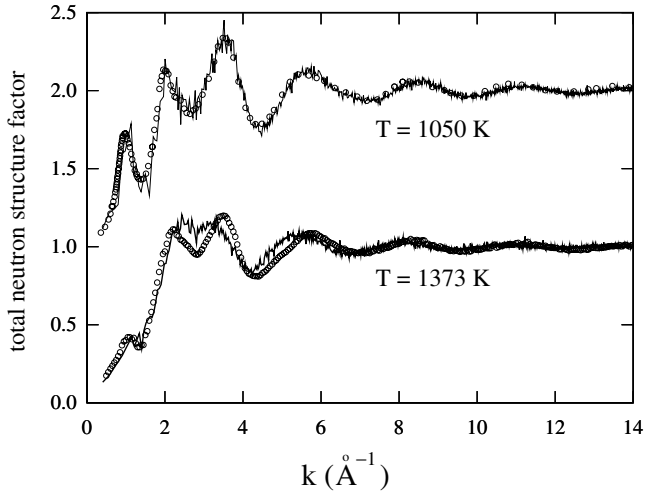

Figure 1. Total neutron structure factors for liquid $GeSe_2$ at $T = 1050$ K and $T = 1373$ K. Open circles: experimental results, from [7] ($T = 1050$ K) and [9] ($T = 1373$ K). Solid line: theory, [14] ($T = 1050$ K) and present calculations ($T = 1373$ K).

2.2 and 5.5 Å^{-1}, where the calculated structure factor is less structured. Our data exhibit a broad maximum for 2.2 Å$^{-1} < k < 3.5$ Å^{-1} which differs from the two distinct peaks found in [9]. This discrepancy can be ascribed to an overstimate of the metallic character of bonding, intrinsic to the DFT scheme, which manifests itself at intermediate compositions within the Ge_xSe_{1-x} liquid family [21]. As shown in [21], where a similar behaviour was found in the case of liquid GeSe, this results in a broader distribution of short Ge–Ge distances, which are systematically larger than in the experiments. These features appear clearly when comparing measured and calculated total pair correlation functions $G_T(r)$ (see figure 2). Theory yields lower and flatter peaks, with the first peak position overestimated by 5% (theory: 2.51 Å, experiment: 2.39 Å). On the basis of what is found in liquid GeSe [21], we conjecture that this difference is mostly due to Ge–Ge interactions and is attenuated by the better agreement existing for the Ge–Se and Se–Se distances.

At shorter wavevectors, the calculated $S_T(k)$ is consistent with experiment. The FSDP, prominent at $T = 1050$ K, has almost disappeared and is reduced to a small shoulder for $k \sim 1$ Å^{-1}. Comparison of the two calculated sets of partial structure factors at $T = 1050$ K and $T = 1373$ K (see figure 3) indicates that this marked decrease is not due to cancellation effects but stems from the absence of a FSDP in any of the three contributions. We notice that the main peak of $S_{GeGe}(k)$ is reduced to a value close to its asymptotic limit. Similarly, the first two maxima in $S_{SeSe}(k)$ become comparable in height and less intense. Since these maxima relate to nearest-neighbour behaviour, these changes reflect a significant alteration of the short-range order among particles of the same species. On the other hand, Ge–Se correlations among nearest neighbours persist in $S_{GeSe}(k)$.

Further insight into the atomic structure is provided by the partial pair correlation functions $g_{\alpha\beta}(r)$, which are shown in figure 4 for $T = 1050$ K [22] and $T = 1373$ K. At $T = 1050$ K the main peak of $g_{GeGe}(r)$ is due to ordering involving Ge atoms in different $GeSe_4$ tetrahedra, with a small tail at distances smaller than 3 Å accounting for a few homopolar bonds. A much larger distribution of distances shows up at $T = 1373$ K involving distances as short as 2.3 Å, together with a barely perceptible first maximum. A lower and broader first peak is

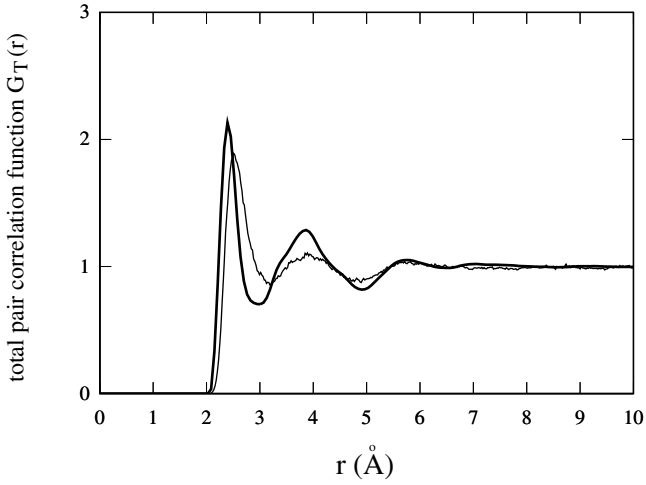

Figure 2. Total pair correlation function $G_T(r)$. Thick line: experiment ([9]). Solid line: our results.

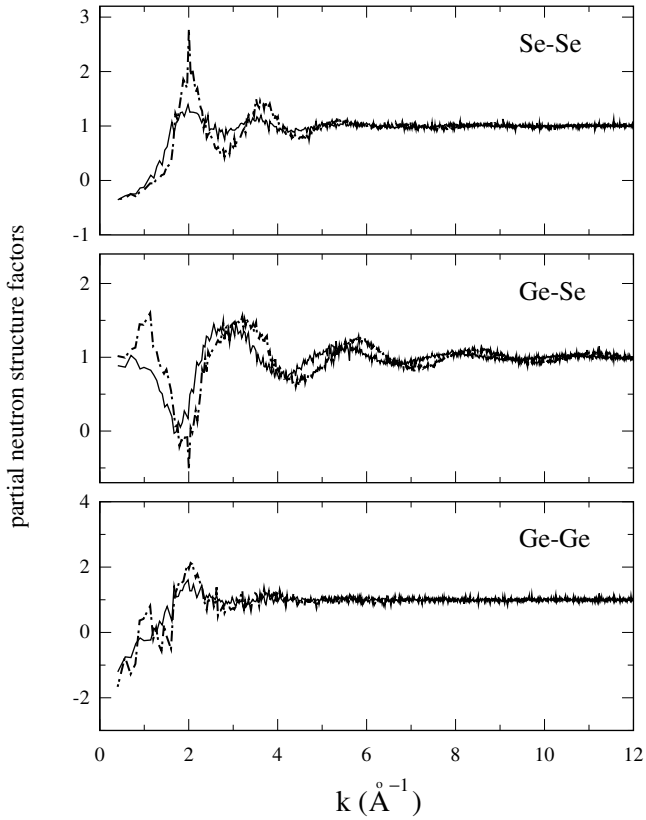

Figure 3. Calculated Faber–Ziman partial structure factors of liquid $GeSe_2$ at $T = 1050$ K (dash–dotted line) and $T = 1373$ K (full line).

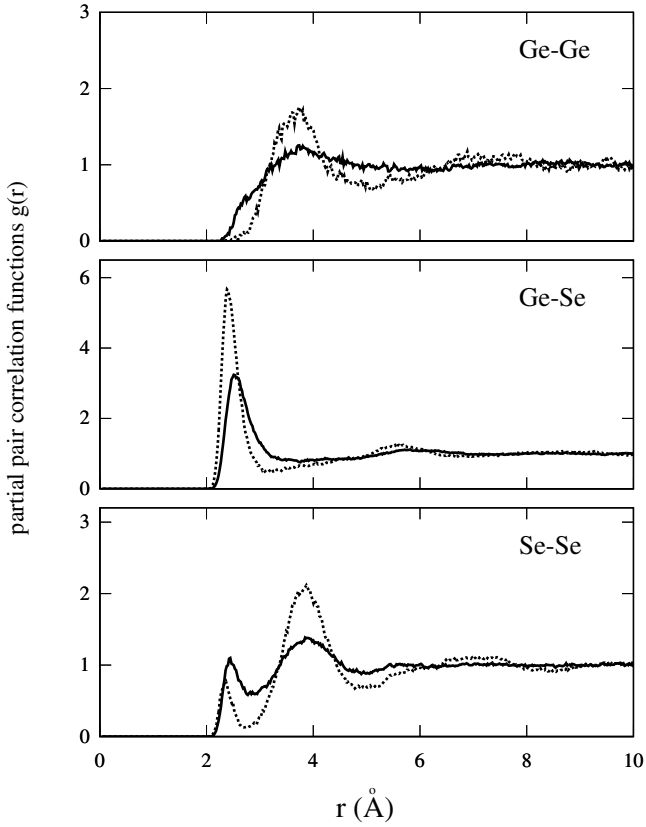

Figure 4. Calculated partial pair correlation functions $g_{\alpha\beta}(r)$ of liquid $GeSe_2$ at $T = 1050$ K (dotted line) and $T = 1373$ K (full line).

also observed in $g_{GeSe}(r)$. In the Se–Se case, the importance of homopolar contacts increases with temperature giving rise to a higher first peak. On the other hand, the second peak which arises from Se–Se interactions among Se atoms sharing Ge neighbours is very much affected by the increased disorder and lowers abruptly.

Table 1. Coordination numbers $n_{\alpha\beta}$ obtained from the $g_{\alpha\beta}(r)$ of liquid $GeSe_2$ at $T = 1050$ K and $T = 1373$ K via integration up to 3 Å. The data for liquid $GeSe_2$ at $T = 1050$ K have been extracted from [22]. The numbers corresponding to the random covalent network (RCN) and chemically ordered network (CON) models are also given.

	n_{GeGe}	n_{GeSe}	n_{SeGe}	n_{SeSe}
$T = 1050$ K	0.14	3.64	1.82	0.46
$T = 1373$ K	0.32	3.19	1.60	1.08
CON	0	4	2	0
RCN	2	2	1	1

These observations can be corroborated by an analysis of the coordination numbers $n_{\alpha\beta}$ relative to the first shell of neighbours given in table 1. These numbers are obtained by integrating the $g_{\alpha\beta}(r)$ up to 3 Å, corresponding to the minimum in the Ge-Se pair-correlation

function at $T = 1050$ K. For comparative purposes, we have included in table 1 the coordination numbers for liquid $GeSe_2$ at $T = 1050$ K and those obtained by applying the random covalent network (RCN) and the chemically ordered network (CON) models to an AX_2 disordered model system [23]. In the RCN model homo- and heteropolar bonds are equally possible, while the CON model maximizes the number of heteropolar bonds and rules out homopolar contacts. While the structure of liquid $GeSe_2$ at both temperatures is definitely very far from a RCN, stronger deviations from chemical order are found in liquid $GeSe_2$ at $T = 1373$ K. The coordination numbers change from 3.78 ($T = 1050$ K) to 3.51 ($T = 1373$ K) for Ge ($n_{GeGe} + n_{GeSe}$) and from 2.28 ($T = 1050$ K) to 2.68 ($T = 1373$ K) for Se ($n_{SeSe} + n_{SeGe}$). We note that the total coordination number defined in [9] as

$$n = c_{Ge}(n_{GeGe} + n_{GeSe}) + c_{Se}(n_{SeSe} + n_{SeGe}) \tag{2}$$

was found to be equal to 2.95, 13% larger than in the experiments (2.6) [9] when calculated for the same integration range (2.09–3.01 Å) at $T = 1373$ K.

Table 2. Upper part: average coordination number $n_{\alpha\beta}^{-fold}(l)$ (expressed as a percentage) for n-fold coordinated Ge atoms (Ge–Ge, Ge–Se, Ge–all) and Se atoms (Se–Ge, Se–Se, Se–all) at a distance of 3 Å, where all refers to an atom irrespective of its identity. For each line, the highest value is given in bold case. Lower part: decomposition of n-fold homopolar coordinated atoms into the average number of dimers, trimers, tetramers and pentamers. Atoms are considered bonded when their separation is smaller than 3 Å.

	One-fold	Two-fold	Three-fold	Four-fold	Five-fold
Ge–Ge (1050 K)	**9.8**	0.2	–	–	–
Ge–Ge (1373 K)	**24.0**	2.5	0.3	–	–
Ge–Se (1050 K)	0.3	6.4	24.6	**63.6**	4.9
Ge–Se (1373 K)	2.3	20.5	**44.6**	28.3	0.4
Ge–all (1050 K)	–	5.2	22.7	**61.8**	9.8
Ge–all (1373 K)	1.1	13.6	**38.3**	36.9	9.4
Se–Se (1050 K)	**31.8**	6.0	0.4	–	–
Se–Se (1373 K)	**42.2**	23.6	4.5	0.4	–
Se–Ge (1050 K)	32.8	**45.2**	14.7	1.4	–
Se–Ge (1373 K)	34.1	**38.7**	13.3	1.1	–
Se–all (1050 K)	3.1	**67.8**	26.5	2.5	–
Se–all (1373 K)	5.0	**42.3**	40.6	10.8	1.1

	dimers	trimers	tetramers	pentamers
Ge (1050 K)	2.0	0.1	–	–
Ge (1373 K)	4.1	0.7	0.2	–
Se (1050 K)	9.1	2.9	0.7	0.2
Se (1373 K)	3.7	11.4	2.1	1.3

The question arises as to whether this enhanced chemical disorder gives rise to a description of the structure intrinsically different from that of the liquid at $T = 1050$ K, where the majority of the Ge atoms are in $GeSe_4$ tetrahedra [14]. We address this issue by calculating the average number $n_{\alpha\beta}^{-fold}(l)$ of Ge and Se atoms l-fold coordinated at 3 Å (see table 2). The quantities $n_{\alpha\beta}$ and $n_{\alpha\beta}^{-fold}(l)$ are simply related by the expression

$$n_{\alpha\beta} = \frac{1}{N_\alpha} \sum_l n_{\alpha\beta}^{-fold}(l)\, l \tag{3}$$

where the sum runs over the l-fold coordinations of the N_α atoms of species α with the atoms of species β. In table 2 we also report the population of homopolar n-mers for the two species. In the case of Ge the number of dimers has doubled at $T = 1373$ K but longer n-mers remain scarce. More striking is the variation in the number of three-fold and four-fold coordinated Ge atoms at high temperature. The largest number is found for three-fold coordinated Ge atoms, especially when bonding with Se atoms only is considered (three-fold Ge–Se, 44.6 % in table 2). The $GeSe_4$ tetrahedron has lost its predominance and is found in percentages close to two-fold coordination (for Ge–Se interactions) and to three-fold coordination (when all atoms are included). Therefore, at high temperature, the $GeSe_4$ tetrahedra fragment by losing one Se atom to give rise to $GeSe_3$ motifs which form further homopolar connections, resulting in Ge–$GeSe_3$ groups. Their existence can also be inferred from table 2, by noticing that high average coordination numbers have been found not only for one-fold Ge–Ge (24.0 %) and three-fold Ge–Se (44.6 %) but also for the four-fold coordination of Ge atoms with any neighbour, irrespective of its identity (four-fold Ge–all, 36.9 %). The same reasoning allows us to conclude that Ge–$GeSe_2$ groups (accounting for the three-fold Ge–all coordinations, 38.3 % in table 2) are present in the system, since in addition to the above mentioned Ge–Ge one-fold coordination, two-fold Ge–Se bonding is far from negligible (20.5%). The formation of these various molecular units is a clear indication of a correlation between the disruption of intermediate-range order and the lack of a prevailing network forming structural motif. The changes occurring to the $n_{\alpha\beta}^{-fold}(l)$ of Se atoms confirm this picture. In addition to the expected two-fold Ge–Se–Ge coordination of Se atoms (two-fold Se–Ge equal to 38.7 % in table 2) we observe that a value as high as 40.6 % is encountered for the three-fold Se–all coordination. This corresponds to a Se atom bonded to two Ge atoms and to one additional Se atom, forming a Se–$SeGe_2$ group, which features one Se–Se homopolar bond.

Overall, our analysis allows us to rationalize the differences between the total neutron structure factors of liquid $GeSe_2$ at two different temperatures and demonstrates that the $GeSe_4$ tetrahedron is not the dominant structural motif for all temperatures studied in [9]. The appearance of the FSDP corresponds to the existence of the prevailing $GeSe_4$ subunit

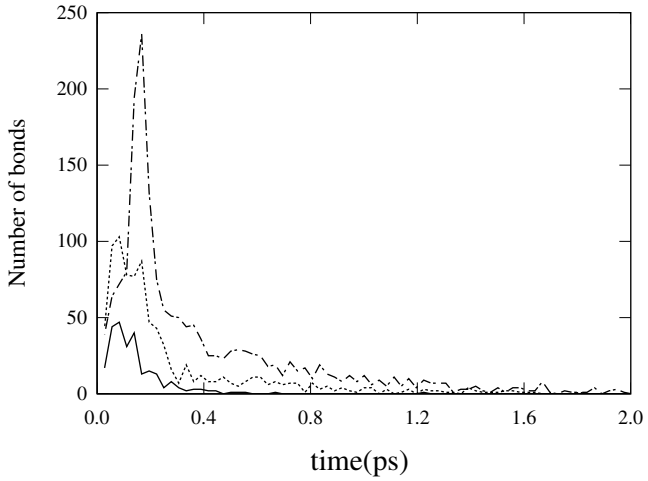

Figure 5. Distribution of bond lifetimes for Ge–Ge bonds (full line), Se–Se bonds (dashed line) and Ge–Se bonds (dash–dotted line). Along the y-axis we report the total number of bonds lasting a time interval given by the corresponding values on the x-axis. A bond is taken to exist as long as the two atoms involved are at a distance shorter than 3 Å.

at $T = 1050$ K. On the other hand, vanishing of the FSDP at $T = 1373$ K results from the coexistence of various structural units which form and recombine frequently and are less stable than the tetrahedron at $T = 1050$ K. This consideration is suggested by the high diffusion coefficients we calculated at $T = 1373$ K (10^{-4} cm^2 s^{-1}) for both Ge and Se atoms (about four times larger than at $T = 1050$ K) and by the distribution of Ge–Ge, Se–Se and Ge–Se bond lifetimes (figure 5). It appears that most bonds do not last more than 0.5 ps, the most stable being the Ge–Se ones.

In conclusion, our calculations have provided an atomic-scale description of the changes occurring in the structure of liquid $GeSe_2$ when the temperature is increased well above $T_m = 1015$ K. The observed breakdown of intermediate-range order is due to the formation of various bonding configurations, none of them standing out and playing the role of the $GeSe_4$ tetrahedron in liquid $GeSe_2$ close to the melting point. Disappearance of the intermediate-range order is strongly related to a marked change in the short-range order, as manifest through an increase in the chemical disorder at the nearest neighbour distance scale.

We acknowledge useful discussions with P S Salmon. CM acknowledges support from the Centre National de la Recherche Scientifique (CNRS) in the framework of the Convention d'Echange France-Suisse. All calculations were performed on the Cray T3E of the Delft Center for High Performance Applied Computing.

References

[1] Susman S, Volin K J, Montague D G and Price D L 1990 *J. Non-Cryst. Solids* **125** 168
[2] Elliott S R 1991 *Nature* **354** 445
[3] Moss S C and Price D L 1985 *Physics of Disordered Materials* ed D Adler, H Fritzsche and S R Ovshinsky (New York: Plenum) p 77
[4] Price D L, Moss S C, Reijers R, Saboungi M L and Susman S 1988 *J. Phys. C: Solid State Phys.* **21** L1069
[5] Salmon P S 1994 *Proc. R. Soc. London* A **445** 351
[6] Wilson M and Madden P A 1994 *Phys. Rev. Lett.* **72** 3033
[7] Penfold I T and Salmon P S 1991 *Phys. Rev. Lett.* **67** 97
[8] Petri I, Salmon P S and Fischer H E 2000 *Phys. Rev. Lett.* **84** 2413
[9] Petri I, Salmon P S and Howells W S 1999 *J. Phys.: Condens. Matter* **11** 10219
[10] Shimojo F, Munejiri S, Hoshino K and Zempo Y 1999 *J. Phys.: Condens. Matter* **11** L153
[11] Shimojo F, Munejiri S, Hoshino K and Zempo Y 2000 *J. Phys.: Condens. Matter* **12** 6161
[12] Vashishta P *et al* 1989 *Phys. Rev. Lett.* **62** 1651
Vashishta P, Kalia R K and Ebbsjö I 1989 *Phys. Rev.* B **39** 6034
[13] Cobb M and Drabold D A 1997 *Phys. Rev.* B **56** 3054
[14] Massobrio C, Pasquarello A and Car R 1998 *Phys. Rev. Lett.* **80** 2342
[15] Massobrio C, Pasquarello A and Car R 1999 *J. Am. Chem. Soc.* **121** 2943
[16] Car R and Parrinello M 1985 *Phys. Rev. Lett.* **55** 2471
[17] Perdew J P, Chevary J A, Vosko S H, Jackson K A, Pederson M R, Singh D J and Fiolhais C 1992 *Phys. Rev.* B **46** 6671
[18] Haye M J, Massobrio C, Pasquarello A, de Vita A, de Leeuw S W and Car R 1998 *Phys. Rev.* B **58** 14661
[19] Ruska J and Thurn H 1976 *J. Non-Cryst. Solids* **22** 277
[20] Waseda Y 1980 *The structure of Non-Crystalline Materials* (New York: McGraw-Hill)
[21] van Roon F H M, Massobrio C, de Wolff E and de Leeuw S W 2000 *J. Chem. Phys.* 5425
[22] Massobrio C, Pasquarello A and Car R 2000 *Comp. Mat. Science* **17** 115
[23] Elliott S R 1990 *Physics of amorphous materials* (London: Longman)